Journal of Experimental Marine Biology and Ecology 461 (2014) 371–380

Contents lists available at ScienceDirect

Journal of Experimental Marine Biology and Ecology

journal homepage: www.elsevier.com/locate/jembe

Current and predicted global change impacts of UVR, temperature and nutrient inputs on photosynthesis and respiration of key marine phytoplankton groups

Marco J. Cabrerizo [a,c,*], Presentación Carrillo [b], Virginia E. Villafañe [c,d], E. Walter Helbling [c,d]

[a] Departamento de Ecología, Facultad de Ciencias, Universidad de Granada, Campus Fuentenueva s/n, 18071 Granada, Spain
[b] Instituto Universitario de Investigación del Agua, Universidad de Granada, C/ Ramón y Cajal, 4, 18071 Granada, Spain
[c] Estación de Fotobiología Playa Unión, Casilla de Correos 15, 9103 Rawson, Chubut, Argentina
[d] Consejo Nacional de Investigaciones Científicas y Técnicas (CONICET), Argentina

ARTICLE INFO

Article history:
Received 8 August 2014
Received in revised form 18 August 2014
Accepted 19 August 2014
Available online xxxx

Keywords:
Nutrients
Photosynthesis dynamics
Phytoplankton
PSII photochemistry
Temperature
UVR

ABSTRACT

Multiple stressors are altering primary production in coastal and estuarine systems; however, it is difficult to predict their combined impacts due to the scarcity of multifactorial experiments. Photosynthesis, respiration, and PSII photochemical performance of *Alexandrium tamarense*, *Chaetoceros gracilis*, *Dunaliella salina* and *Isochrysis galbana* were studied during daily cycles using a combination of two radiation treatments (UVR + PAR and PAR), two nutrient concentrations, and three temperatures (14, 17 and 20 °C). UVR exerted a negative impact in all species decreasing photosynthesis and quantum yield of PSII under low nutrient concentrations and temperatures up to 20 °C. At higher temperatures (global change scenario of 4 °C increase) and increased UVR and nutrients, *C. gracilis* and *I. galbana* reversed their responses by increasing photosynthesis and repair rates, respectively; they also showed a decrease in respiration rates. In contrast, *A. tamarense* and *D. salina* showed further decrease in photosynthesis and repair rates compared to present conditions. Our modeled responses to warming under a scenario of increased nutrients and UVR suggest that diatoms and haptophytes will benefit from these conditions and possibly will outcompete chlorophytes and dinoflagellates. If this is a generalized response, it might influence primary production and affect food web interactions in coastal ecosystems.

1. Introduction

Phytoplankton is responsible for ca. 50% of the global primary production (Field et al., 1998) and coastal systems, including estuaries, are among the most productive areas of the planet (Cloern et al., 2014); therefore, coastal phytoplankton has been the focus of many investigations aiming to understand the effects of multiple stressors associated to global change (Kennish et al., 2014). Many studies were devoted to evaluate the effects and impacts of higher fluxes of ultraviolet radiation (UVR, 280–400 nm), either due to depletion of the ozone layer or as the result of increased stratification (Häder et al., 2011; Helbling and Zagarese, 2003; McKenzie et al., 2011); the increase in surface seawater temperature associated to global warming (Häder et al., 2011; Luo et al., 2008; Winder and Sommer, 2012); and the increase of nutrient inputs into coastal marine ecosystems by rivers or atmospheric deposition due, in turn, to increased rainfall and/or stronger and more frequent wind events (IPCC, 2013).

It is already known that UVR produces negative effects on phytoplankton e.g., by affecting photosynthesis and respiration (Beardall and Raven, 2004; Beardall et al., 1997) and damaging vital cellular targets such as the DNA molecule (Buma et al., 2003), proteins and membrane lipids (Abo-Shady et al., 2008; Arts and Rai, 1997; Guihéneuf et al., 2010; Skerratt et al., 1998). However UV-A (315–400 nm) has been shown to stimulate photosynthesis under low photosynthetic active radiation (PAR, 400–700 nm) or under fast mixing (Barbieri et al., 2002; Helbling et al., 2003), and has also been involved in photorepairing UV-B (280–315 nm)-induced DNA damage (Buma et al., 2003). Higher nutrient inputs, on the other hand, generally benefit primary production (Lagaria et al., 2011), increase growth of algae (Toseland et al., 2013) and decrease photoinhibition (Bergmann et al., 2002); although it has also been reported that high nutrients unmask the negative UVR-effects on algal development (Carrillo et al., 2008; Korbee et al., 2012). Recent studies have determined variable effects of increased temperature, increasing maximum quantum yield of PSII in the dinoflagellate *Symbiodinium* sp. (Takahashi et al., 2013), producing shifts towards smaller-sized species (Thomas et al., 2012)

* Corresponding author at: Departamento de Ecología, Facultad de Ciencias, Universidad de Granada, Campus Fuentenueva s/n, 18071 Granada, Spain. Tel.: +34 958 24 10 00x20007.
E-mail addresses: mjc@ugr.es (M.J. Cabrerizo), pcl@ugr.es (P. Carrillo), virginia@efpu.org.ar (V.E. Villafañe), whelbling@efpu.org.ar (E. Walter Helbling).

http://dx.doi.org/10.1016/j.jembe.2014.08.022
0022-0981/

or reducing UVR-induced photoinhibition in the diatom *Thalassiosira pseudonana* (Sobrino and Neale, 2007). This is probably due to the increases in depoxidation rate of the xantophyll pigment cycle and consequently higher repair rates of PSII (Dimier et al., 2009; Kulk et al., 2013) or higher RUBISCO activity (Helbling et al., 2011). In contrast, increased temperature resulted in inhibition of growth of some tropical diatoms (Halac et al., 2013) and exacerbated the harmful UVR effects on effective photochemical quantum yield in some sub-Antarctic brown-algae (Cruces et al., 2013). These contrasting findings are due not only to different experimental conditions, but also to the species-specificity of responses. Moreover, the effects of a single factor (or stressor) on a particular organism or process is usually different from when considered in combination with other factors, due to the antagonistic or synergistic nature of interactions (Folt et al., 1999). Another potential cause of differences in responses to multiple stressors lies on the evolutionary traits achieved through time i.e., allowing acclimation, that in turn result in differential sensitivity to changing environmental factors.

The aim of this study is to evaluate the photosynthetic and respiratory responses, together with PSII photochemical activity, of key marine phytoplankton species, representatives of four different phytoplankton phyla, under the combination of UVR, temperature and nutrients, considering a global change context. In particular, it was hypothesized that a combined increase in temperature and nutrients will exacerbate the potential negative UVR-effects on photosynthesis–respiration and photochemical activity on phytoplankton compared with current ambient conditions. To test this hypothesis, experiments were carried out in which monospecific cultures of different phytoplankton groups characteristic of coastal areas were exposed to different combinations of variables associated to global change i.e., two radiation, two nutrients and three temperature conditions and the photosynthetic/photochemical and respiratory responses during short term incubations were followed. The data obtained, in turn, allowed predicting the responses of key phytoplankton species in a future global change scenario as expected by year 2100 (IPCC, 2013).

2. Material and methods

2.1. Culture conditions

Experiments were carried out during the Austral Autumn (March–June, 2013). The phytoplankton species used in this study were isolated from the Patagonian coast and maintained in the Algal Culture Collection of Estación de Fotobiología Playa Unión (EFPU). The dinoflagellate *Alexandrium tamarense* (Lebour) Balech, the diatom *Chaetoceros gracilis* Schütt, the chlorophyte *Dunaliella salina* (Dunal) Teodoresco and the haptophyte *Isochrysis galbana* Parke were grown and maintained in exponential growth (chlorophyll *a* values ranging between 50 and 60 μg l^{-1}) in either a high-nutrient (f/2) (hereafter HN) or a low-nutrient (f/40) medium (hereafter LN) (Guillard and Ryther, 1962), under three experimental temperatures, 14 °C, 17 °C and 20 °C, inside an environmental illuminated chamber (Minicella, Argentina). Control treatments of nutrient and temperature represent the mean values of either the contributions of nitrate, nitrite, phosphate and silicate of the Chubut River during low-tide (f/40) and the average sea water temperatures (14 °C) through end-March to mid-May (Helbling et al., 1992, 2010).

Semi-continuous cultures were maintained in non-aerated 1-l bottles, filled up to 50% of their volume and maintained in exponential growth by diluting them every day with 250 ml of fresh medium to maintain the initial volume. The cultures were pre-acclimated for seven days to both temperature and nutrient conditions as described above before being used in experimentation. During this acclimation period the cultures grew under a 12 h L:12 h D photoperiod, under illumination provided by fluorescent tubes (Phillips daylight), receiving 300 μmol photons m^{-2} s^{-1} of photosynthetic active radiation (PAR, 400–700 nm).

2.2. Experimental set-up

In order to assess the combined impact of UVR (i.e., factor Rad), nutrient (i.e., factor Nut) and temperature (i.e., factor Temp) on the four species (i.e., factor Spp) considered in this study, a $2 \times 2 \times 3 \times 4$ matrix was implemented. Triplicate samples for each radiation and nutrient condition were placed into 40 ml round quartz vessels for measurements of photosynthesis and respiration, while another set of triplicate samples was placed in 40 ml quartz tubes to measure fluorescence parameters. The two radiation treatments were: (1) PAB, with samples receiving UVR + PAR (>280 nm), uncovered quartz tubes, and (2) P, with samples receiving only PAR (>400 nm), quartz tubes covered with Ultraphan film (UV Opak 395 filter, Digefra). The two nutrient treatments consisted in HN and LN media, while the three temperature treatments were 14, 17 and 20 °C, as mentioned above for the pre-acclimation period. The samples were placed in an illuminated culture chamber (Sanyo MLR-350, Japan) that kept the wanted temperature constant, while the radiation conditions were provided by 10 Philips daylight fluorescent tubes for PAR and 5 tubes Q-Pannel UVA-340 for UVR. The cultures were exposed to irradiances of 164.1 (754.9 μmol photons m^{-2} s^{-1}), 42.8, and 0.7 W m^{-2} for PAR, UV-A and UV-B, respectively, which represent the mean daily values for the experimental period (Helbling et al., 2005). The spectral output of the lamps was checked with a spectroradiometer (Ocean Optics model HR 2000CG-UV-NIR), and no UV-C radiation output was measured. The radiation exposure period lasted 6 h in order to get a radiation dose comparable with natural daily doses during the period of experimentation. Therefore samples received a daily dose of 3.5 MJ m^{-2} for PAR, 910 kJ m^{-2} for UV-A and 15 kJ m^{-2} for UV-B. After exposure, the cultures were maintained inside the chamber for another 8 h in darkness; this time period was chosen based on preliminary measurements, and also to obtain various data points to calculate respiration.

3. Analysis and measurements

3.1. Photosynthesis and respiration measurements

Oxygen concentration was measured using a Presens system (PreSens GmbH, Germany) consisting of sensor-spot optodes (SP-PSt3-NAU-D5-YOP) and an optic-fiber oxygen transmitter (Fibox 3) connected to a computer equipped with an Oxyview 6.02 software to register the data. The system was calibrated by a two-point calibration, together with data of atmospheric pressure and temperature before each experiment, following the manufacturer's recommendations. Measurements were made at the initial time (t_0) and then every hour during the 6 h of exposure to artificial radiation, every 30 min during the first 2 h of darkness, and then every 1.5 h until the end of the dark period (8 h).

3.2. PSII fluorescence measurements

In vivo photochemical parameters were obtained using a pulse amplitude modulated (PAM) fluorometer (Walz, Water PAM, Effeltrich, Germany). Aliquots of 3 ml of sample were taken every 15 min during the first hour of exposure, and then with the same periodicity as mentioned before for oxygen measurements; the samples were placed in a cuvette, and measured six times immediately after sampling, without any dark-adaptation. The quantum yield of PSII (Φ_{PSII}) was calculated using the equations of Genty et al. (1989) and Maxwell and Johnson (2000) as:

$$\Phi_{PSII} = \Delta F / F'_m = (F'_m - Ft) / F'_m$$

where F'_m is the maximum fluorescence induced by a saturating light pulse (ca. 5300 μmol photons m^{-2} s^{-1} in 0.8 s) and F_t is the current steady state fluorescence induced by a weak actinic light of ~492 μmol photons m^{-2} s^{-1} in light-adapted cells.

The non-photochemical quenching (NPQ) of chlorophyll *a* (Chl-*a*) fluorescence, used as a proxy of the dissipation of the excess light energy, was obtained directly using the PAM fluorometer. The software stores the F_m value that is then used with every sample to calculate the NPQ. In this study F_m values for each species were determined and stored every time just before any exposure to solar radiation using a few dark-acclimated samples, and thus the NPQ data obtained with the PAM software based on these values were routinely used. Previous studies carried out by our group (Halac et al., 2010) showed that there were no significant differences between NPQ values calculated when F_m was determined for each individual sample and those obtained directly using the PAM fluorometer software.

3.3. Chlorophyll-a concentrations and UV-absorbing compounds

Aliquots of 50 ml of sample were filtered onto GF-C filters (Munktell, Sweden) and photosynthetic pigments and UV-absorbing compounds were extracted in 5 ml of methanol. The tubes containing the methanolic extract were firstly sonicated at 20 °C for 20 min, followed by 40 min of extraction. After this, the samples were centrifuged for 20 min at 2000 rpm and the absorption spectra of the supernatant were obtained by doing scans between 250 and 750 nm with a spectrophotometer (Hewlett Packard, model HP 8453E). Chl-*a* concentration was calculated with the equation of Porra (2002) and the same sample was used to calculate Chl-*a* concentration from the fluorescence of the extract (Holm-Hansen and Riemann, 1978) before and after acidification (1 N HCl) using a fluorometer (Turner Designs, model TD 700). There were no differences between Chl-*a* concentrations determined by the two methods, thus values calculated with the equation of Porra (2002) were used. Once the scans (250–750 nm) for UV-absorbing compounds (UVAC) were obtained, the raw data were processed using a baseline correction and considering the entire area delimited under the peak at 337 nm and the peak height. Since both values gave similar information, the peak height at 337 nm was used as previously described in Helbling et al. (1996).

3.4. Data and statistical analysis

Photosynthesis and respiration rates (in μmol O_2 μg Chl-a^{-1} h^{-1}) were calculated as the slope of the regression line of chlorophyll-specific oxygen concentrations versus time.

The net UVR effect on photosynthesis and/or respiration was calculated as:

$$\text{UVR effect} = [O_2]_{PAB} - [O_2]_P,$$

where $[O_2]_{PAB}$ is the photosynthesis or respiration rate in the PAB-treatment, and $[O_2]_P$ is the photosynthesis or respiration rate in the P-treatment.

Inhibition (k — in min^{-1}) and recovery (r — in min^{-1}) rates were estimated as the decrease and increase, respectively, in Φ_{PSII} by applying an exponential regression fit during the radiation exposure (inhibition) and darkness (recovery) periods to the data:

$$\Phi_{PSII} = A * e^{-kt} \text{ or}$$
$$\Phi_{PSII} = A * e^{rt}$$

where Φ_{PSII} is the quantum yield of PSII, A is a constant, k/r represents inhibition/recovery, respectively, and t is the time.

The net UVR effect on k and r of PSII was calculated as:

$$\text{UVR effect} = (k)_{PAB} - (k)_P$$

$$\text{UVR effect} = (r)_{PAB} - (r)_P$$

where k and r are the mean values of inhibition and recovery, respectively, for any of the measurements done in the PAB and P radiation treatments.

A four-way analysis of variance (ANOVA) was used to determine interactions among radiation, nutrients, temperature and species on photosynthesis, respiration, inhibition and recovery rates. The normality (by Shapiro–Wilk's W test or Kolgomorov–Smirnov) and homoscedasticity (using Cochran, Hartley & Bartlett or Levene's tests) were checked for each data group before the ANOVA application. A post hoc test (Fisher's least significant difference) was used to determine significant differences within and among the different factors. A 95% confidence limit was used in all tests and all analyses were performed with the STATISTICA v7.0 software (Statsoft Inc., 2005).

Based on the photosynthesis and respiration rates, the UVR effect for each experimental condition for each species was calculated, and such values were fitted using a polynomial model. Error propagations were used to calculate the variance of the UVR effects. The model was also used to extend a prediction of the combined effects of temperature and nutrients at temperatures higher than the experimental 20 °C used in our study (i.e., up to 24 °C).

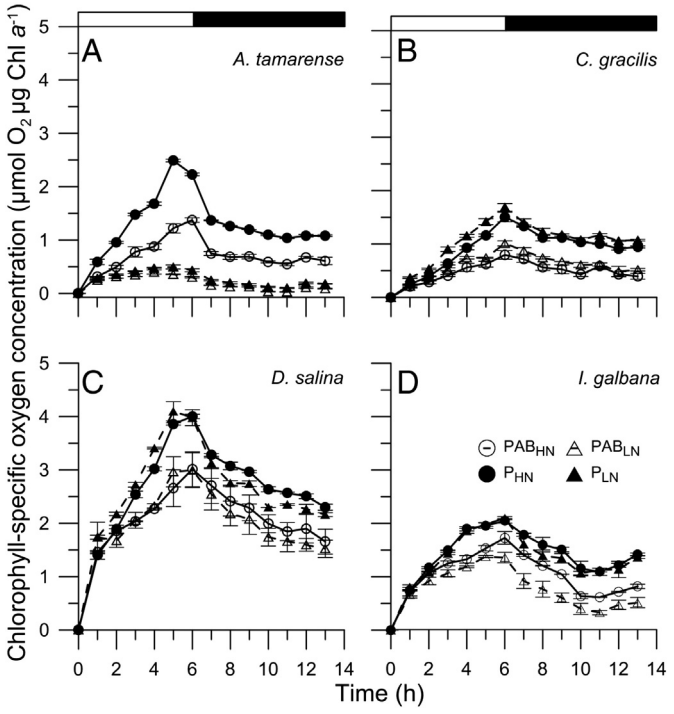

Fig. 1. Mean chlorophyll-specific oxygen concentration (in μmol O_2 μg Chl a^{-1}) of *Alexandrium tamarense* (A), *Chaetoceros gracilis* (B), *Dunaliella salina* (C) and *Isochrysis galbana* (D) during 6 h exposure to UVR + PAR (PAB, open symbols) and PAR only (P, black symbols), and 8 h of darkness at 17 °C. The horizontal white and black bars on the top indicate the radiation (exposure) and dark periods, respectively. Samples were grown and incubated at high (HN, circles) and low nutrient (LN, triangles) conditions. Each symbol represents the mean of triplicate samples while the vertical lines indicate the standard deviation.

4. Results

4.1. Dynamics of photosynthesis and respiration

Representative data of oxygen evolution (i.e., production and respiration) at 17 °C, normalized to the initial Chl-*a* concentration, for the four species studied are shown in Fig. 1 (only this temperature is shown for simplicity, as the trends were similar at 14, 17 and 20 °C). For all species, the general pattern was of an increase in chlorophyll-specific photosynthesis (i.e., production) during the radiation exposure period, whereas the concentration was reduced (i.e., respiration) towards stabilization during the dark period. However, the responses were clearly species-specific, according to the radiation and nutrient treatments imposed to the samples. Overall, two clear and distinct patterns were observed: In the case of *A. tamarense* (Fig. 1A), nutrient concentration had greater impact on photosynthesis than radiation conditions, resulting in higher O_2 concentrations in cells grown under HN, regardless of the radiation treatment. On the other hand, as in the cases of *C. gracilis* (Fig. 1B), *D. salina* (Fig. 1C), and *I. galbana* (Fig. 1D), radiation exposure caused more significant effects than nutrient concentration, and thus samples incubated under the P-treatment had higher oxygen concentration than those under the PAB-treatment, regardless of the nutrient concentration.

The species-specific responses to each variable and condition are best seen in the rates of photosynthesis and respiration (Fig. 2). There were significant interactions between factors (i.e., Rad × Nut; Rad × Temp; and Nut × Temp) with the exception of Rad × Nut on respiration (Table 1). For *A. tamarense* (Fig. 2A) and under HN treatment, photosynthesis rates were higher at high temperatures (20 °C), with values of ~0.36 and 0.44 μmol O_2 μg Chl a^{-1} h^{-1} under PAB and P, respectively; an opposite trend was observed under LN conditions, with photosynthesis rates being lower at high temperatures. Similar

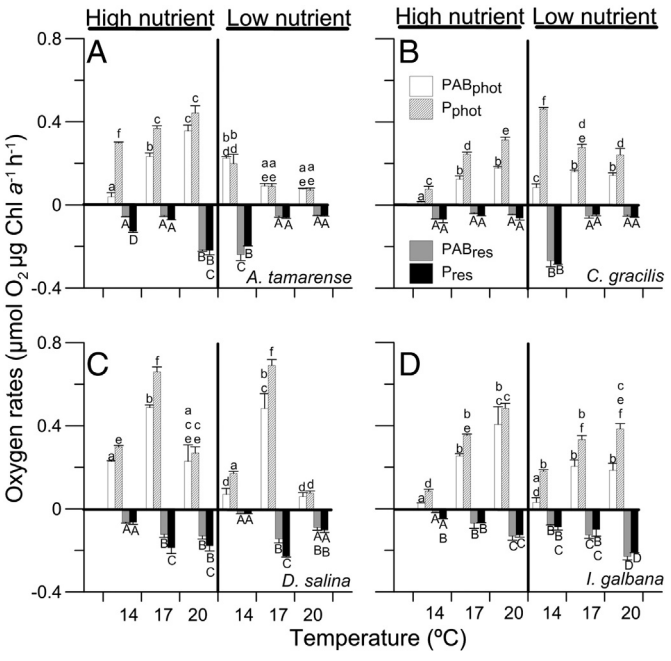

Fig. 2. Rates (in μmol O_2 μg Chl a^{-1} h^{-1}) of photosynthesis (positive values) and respiration (negative values) of *Alexandrium tamarense* (A), *Chaetoceros gracilis* (B), *Dunaliella salina* (C) and *Isochrysis galbana* (D). Samples were grown and incubated at high (HN) and low nutrient (LN) conditions; three temperatures: 14, 17, and 20 °C, and exposed to two radiation treatments: UVR + PAR (PAB, white and gray bars) and PAR only (P, dashed and black bars). The lines on the top of the bars indicate the standard deviation. Significance of post hoc comparisons between radiation treatments for each nutrient condition and temperature is represented with small and capital letters for production and respiration rates, respectively.

Table 1
Results of statistical analysis for the effects of radiation (Rad), nutrients (Nut), temperature (Temp), and species (Spp), and their interactions, on photosynthesis and respiration. All *F* values are rounded to two significant digits. Radiation (PAB and P), nutrient (HN and LN), and temperature (14, 17 and 20 °C). df, degrees of freedom; n.s., not significant.

Treatment	df	Photosynthesis		Respiration	
		F	p	*F*	p
Radiation	1	104.08	<0.001	6.38	<0.05
Nutrient	1	21.78	<0.001	21.42	<0.001
Temperature	2	57.72	<0.001	15.96	<0.001
Specie	3	23.88	<0.001	15.93	<0.001
Rad * Nut	1	0.19	n.s.	4.57	<0.05
Rad * Temp	2	4.15	<0.05	0.33	n.s.
Nut * Temp	2	40.99	<0.001	48.62	<0.001
Rad * Spp	3	1.59	n.s.	1.99	n.s.
Nut * Spp	3	18.90	<0.001	29.12	<0.001
Temp * Spp	6	32.88	<0.001	69.31	<0.001
Rad * Nut * Temp	2	0.65	n.s.	0.33	n.s.
Rad * Nut * Spp	3	3.01	<0.05	1.77	n.s.
Rad * Temp * Spp	6	2.62	<0.05	3.39	<0.01
Rad * Temp * Spp	6	4.82	<0.001	26.71	<0.001
Rad * Nut * Temp * Spp	6	1.97	n.s.	1.76	n.s.

to photosynthesis, absolute respiration rates were somehow higher at 20 °C under HN conditions whereas they were lower at higher temperature under LN conditions. *C. gracilis* (Fig. 2B) under HN conditions showed an increase in production rates with increasing temperature; however the highest production (~0.46 μmol O_2 μg Chl a^{-1} h^{-1}) was determined at 14 °C in the LN treatment. For this species, and under HN conditions, no significant changes were observed in absolute respiration rates; however, they were lower with increasing temperature at LN conditions. In *D. salina* (Fig. 2C) photosynthetic rates were significantly lower at 14 and 20 °C as compared to 17 °C in both nutrient conditions. In this species, absolute respiration rates were higher at high temperatures in the HN condition, and maximal values were determined at 17 °C under LN conditions. Finally, *I. galbana* (Fig. 2D) exhibited a clear trend of increasing photosynthesis rates with increasing temperature under both nutrient conditions. Absolute respiration rates were also higher with increasing temperature in both nutrient conditions.

For all species UVR had, in general, a negative impact on photosynthesis rates, under both nutrient conditions, up to 20 °C (Fig. 3A, B, dotted area). The responses at higher predicted temperatures varied among species with (i) an antagonistic effect among UVR and temperature on *D. salina*, with increasing temperatures counteracting the negative UVR effect under both nutrient conditions (Fig. 3A, B). A similar effect was observed in *A. tamarense* under the LN condition (Fig. 3A) and *I. galbana* under the HN condition (Fig. 3B); (ii) a synergistic effect of temperature and UVR in *C. gracilis* and *I. galbana* under LN (Fig. 3A, dotted area) and for *A. tamarense* and *C. gracilis* under HN (Fig. 3B, dotted area). Overall, at predicted increased temperatures, high nutrient inputs together with UVR would benefit the photosynthesis of *C. gracilis* and *I. galbana*, while they would decrease the photosynthesis of *A. tamarense* and *D. salina* (Fig. 3C, striped bar). In the case of respiration (Fig. 3D, E and F), the four species would have a continuous increase of UVR impact under predicted higher temperatures and under LN conditions (Fig. 3D, striped bar), being this effect more accentuated in *C. gracilis*. In contrast, little effect as compared to current conditions would be observed under HN conditions for all species (Fig. 3E). Finally, and in contrast to photosynthesis, the net effect of UVR and high nutrients would exert a positive effect on respiration, decreasing it significantly in all cases, with the exception of *I. galbana* where it would be slightly increased (Fig. 3F).

4.2. Dynamics of photochemical parameters

The dynamics of the quantum yield of PSII (Φ_{PSII}) for the four species studied showed a similar behavior at 17 °C (only this temperature is

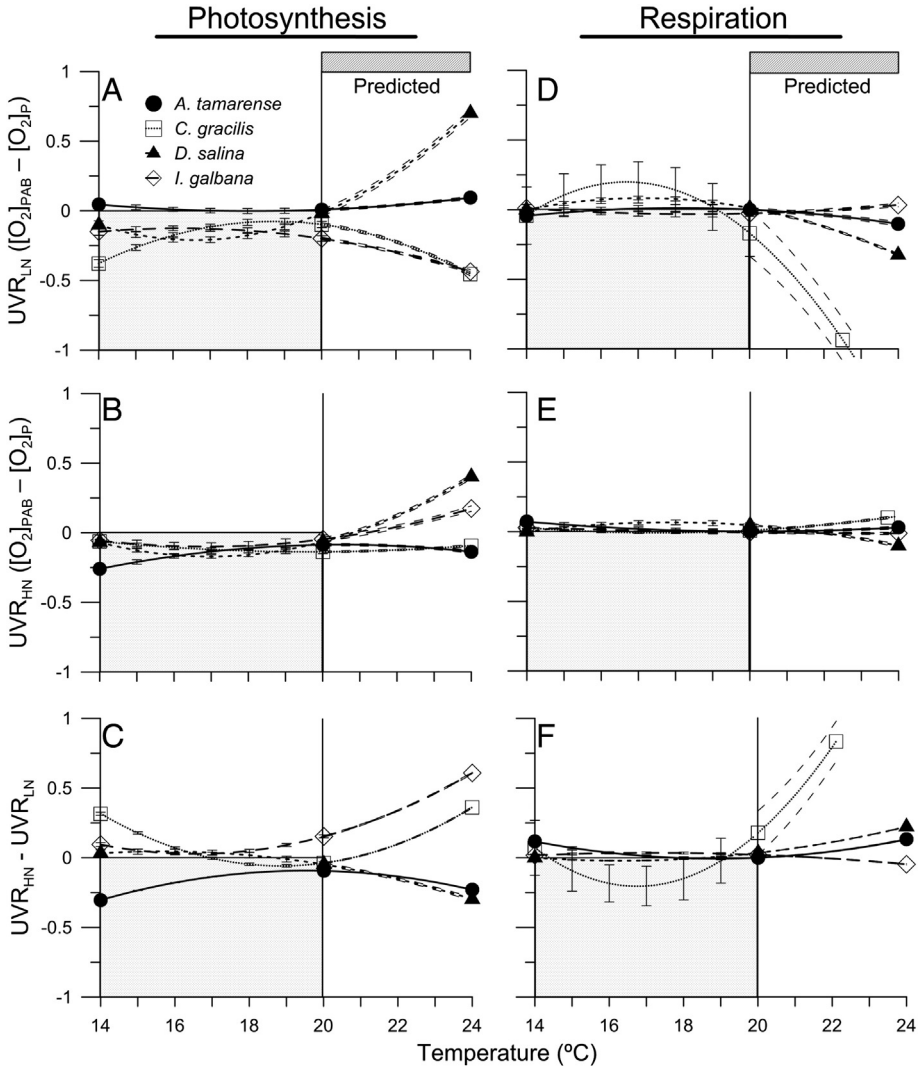

Fig. 3. UVR effect, evaluated as the difference between PAB and P treatments, on photosynthesis (A, B) and respiration (D, E) rates as a function of temperature, for *Alexandrium tamarense* (circles), *Chaetoceros gracilis* (squares), *Dunaliella salina* (triangles), and *Isochrysis galbana* (diamonds) within the experimental temperature interval (temperatures up to 20 °C) and within the increased temperature (i.e., predicted values, temperatures up to 24 °C). Samples were grown and incubated at high (HN) and low nutrient (LN) conditions, and three temperatures, 14, 17, and 20 °C. The net effect of high nutrients under UVR within the experimental (temperatures up to 20 °C) and predicted temperature interval (i.e., predicted values, temperatures up to 24 °C) on photosynthesis (C) and respiration (F) is shown. The lines (solid and broken) represent the best fit using a polynomial function, while the vertical lines represent 95% confidence intervals, shown every 1 °C in the 14–20 °C interval and continuously in the 20–24 °C interval.

shown for simplicity, as the trends were similar at 14, 17 and 20 °C) (Fig. 4). All species displayed a decrease in Φ_{PSII} as soon as the radiation exposure started, with values remaining low during the exposure, followed by a partial or total recovery in darkness. In general, and although there was some variability in the responses among species, radiation was the factor that most affected Φ_{PSII}, with values under P being higher than those under the PAB-treatment, regardless of the nutrient conditions. Based on the decrease and recovery of Φ_{PSII}, the inhibition (k) and recovery (r) rates (in min^{-1}) for all species under the different treatments were calculated (Fig. 5). As expected, significant variability among species and treatments was determined. The general trend, however, was of higher absolute k values as compared to r, and also of higher values under the PAB as compared to P treatments, for any temperature and nutrient condition. A significant interaction Rad × Nut × Temp × Spp on k and r was found (Table 2). For *A. tamarense* (Fig. 5A) absolute k and r values decreased with increasing temperature under HN, whereas the opposite occurred under LN. For *C. gracilis* (Fig. 5B) and *I. galbana* (Fig. 5D) there was a general trend of decreasing inhibition with increasing temperature under both nutrient conditions, except for *C. gracilis* grown at LN that had similar inhibition at all temperatures. In regard to recovery rates of *C. gracilis* and *I. galbana*, there were in general no significant differences among temperatures under both nutrient conditions. Finally, in the case of *D. salina* (Fig. 5C), the inhibition increased with temperature under both nutrient conditions, while there were no differences in recovery rates.

Fig. 6 shows a representative example of the variations in non-photochemical quenching (NPQ) throughout the radiation exposure and recovery in darkness. In general, NPQ showed somehow opposite responses as Φ_{PSII} (Fig. 4), with increasing values during the radiation exposure period, and decreasing during darkness. There was important species-specific variability in NPQ responses, as seen in samples incubated at 17 °C (Fig. 6). Higher NPQ values were determined in *A. tamarense* (Fig. 6A) and *D. salina* (Fig. 6C) in samples under LN as compared to those under HN. In contrast, *C. gracilis* (Fig. 6B) had higher NPQ values in samples grown under HN as compared to those under LN conditions. Finally, in *I. galbana* (Fig. 6D), a strong radiation effect was determined, with high NPQ values in samples under the PAB treatment, regardless of the nutrient condition. Overall, the lowest NPQ values were determined in samples either under HN (i.e., *A. tamarense*,

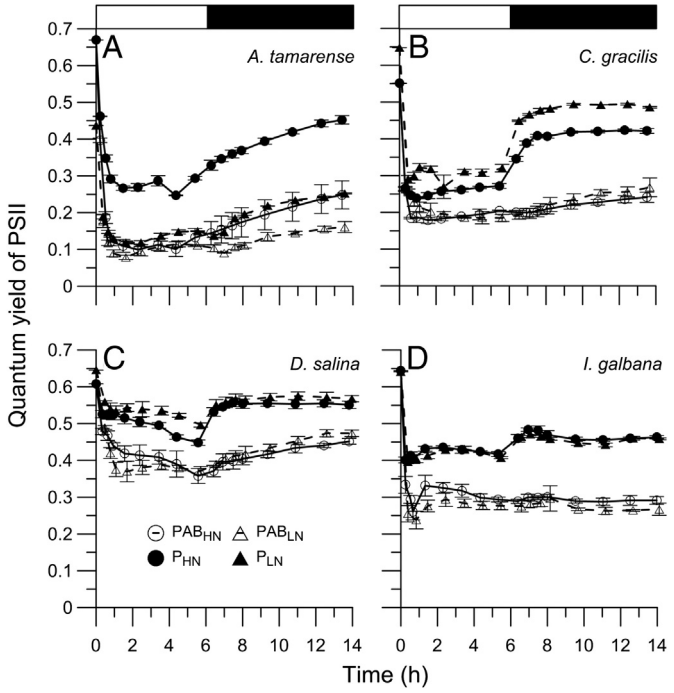

Fig. 4. Mean effective photochemical quantum yield (Y) of *Alexandrium tamarense* (A), *Chaetoceros gracilis* (B), *Dunaliella salina* (C) and *Isochrysis galbana* (D) during the 6 h exposure to UVR + PAR (PAB, open symbols) and PAR only (P, black symbols), and 8 h of darkness. The horizontal white and black bars on the top indicate the radiation (exposure) and dark periods, respectively. Samples were grown and incubated at high (HN, circles) and low nutrient (LN, triangles) conditions. Each symbol represents the mean of triplicate samples while the vertical lines indicate the standard deviation.

Table 2
Results of statistical analysis for the effects of radiation (Rad), nutrients (Nut), temperature (Temp), and species (Spp), and their interactions on inhibition and recovery of the effective photochemical quantum yield. All *F* values are rounded to two significant digits. Radiation (PAB and P), nutrient (HN and LN), and temperature (14, 17 and 20 °C). df, degrees of freedom; n.s., not significant.

Treatment	df	Inhibition (*k*)		Recovery (*r*)	
		F	p	*F*	p
Radiation	1	201.00	<0.001	3.28	n.s.
Nutrient	1	16.50	<0.001	0.00	n.s.
Temperature	2	10.86	<0.001	1.38	n.s.
Specie	3	36.07	<0.001	1.80	n.s.
Rad ∗ Nut	1	5.75	<0.05	0.23	n.s.
Rad ∗ Temp	2	2.23	n.s.	0.07	n.s.
Nut ∗ Temp	2	5.92	<0.01	3.89	<0.05
Rad ∗ Spp	3	18.73	<0.001	4.30	<0.01
Nut ∗ Spp	3	11.32	<0.001	10.72	<0.001
Temp ∗ Spp	6	58.98	<0.001	20.63	<0.001
Rad ∗ Nut ∗ Temp	2	0.32	>0.05	4.60	<0.05
Rad ∗ Nut ∗ Spp	3	3.00	<0.05	13.61	<0.001
Rad ∗ Temp ∗ Spp	6	8.81	<0.001	5.92	<0.001
Rad ∗ Temp ∗ Spp	6	7.75	<0.001	2.18	n.s.
Rad ∗ Nut ∗ Temp ∗ Spp	6	2.72	<0.05	8.36	<0.001

Fig. 6A and *D. salina*, Fig. 6C) and LN (i.e., *C. gracilis*, Fig. 6B) or under the P-treatment (i.e., *I. galbana*, Fig. 6D).

To estimate the effectiveness of NPQ as a mechanism to cope with excess energy, the rates of inhibition (*k*) vs. NPQ values were compared for the different temperature and nutrient treatments (data not shown). It was observed that for *A. tamarense*, *C. gracilis* and *I. galbana* under the PAB-treatment and grown under HN conditions as well as *I. galbana* under LN conditions, higher inhibition with decreasing temperature was associated to increasing NPQ values. This pattern was not clear in

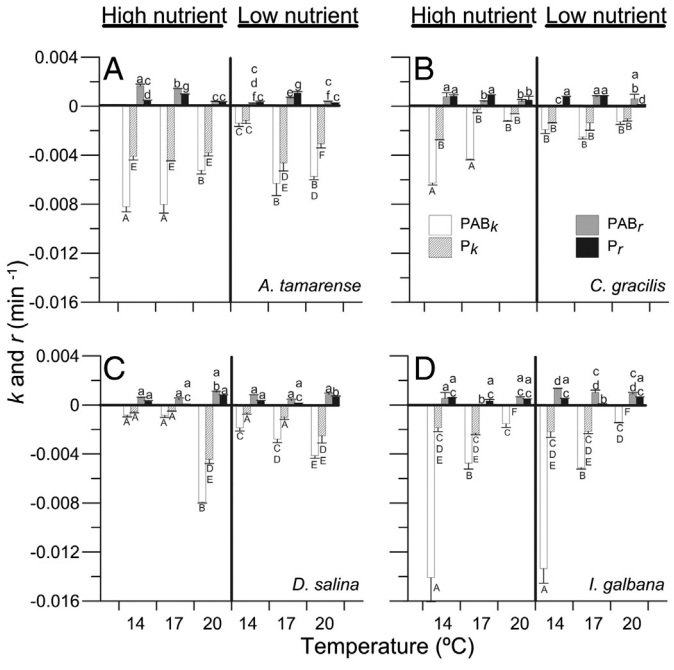

Fig. 5. Inhibition (*k*) (negative values) and recovery (positive values) (*r*) rates (in min^{-1}) of *Alexandrium tamarense* (A), *Chaetoceros gracilis* (B), *Dunaliella salina* (C) and *Isochrysis galbana* (D). Samples were grown and incubated at two nutrient conditions, HN and LN; three temperatures: 14, 17, and 20 °C, and exposed to two radiation treatments: UVR + PAR (PAB, white and gray bars) and PAR only (P, dashed and black bars). The lines on the top of the bars indicate the standard deviation. Significance of post hoc comparisons between radiation treatments for each nutrient condition and temperature is represented with small and capital letters for *r* and *k* rates, respectively.

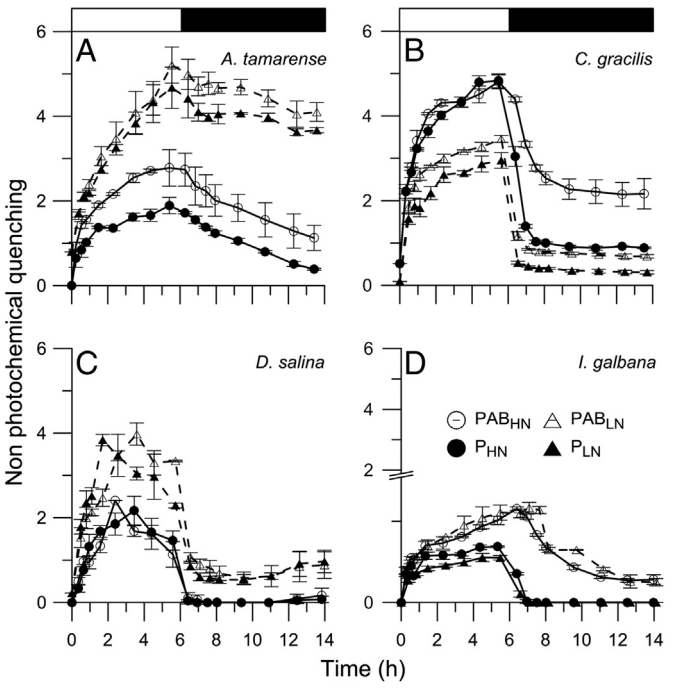

Fig. 6. Mean non photochemical quenching (NPQ) of *Alexandrium tamarense* (A), *Chaetoceros gracilis* (B), *Dunaliella salina* (C) and *Isochrysis galbana* (D) during the 6 h of exposure to UVR + PAR (PAB, open symbols) and PAR only (P, black symbols), and 8 h of darkness. The horizontal white and black bars on the top indicate the radiation (exposure) and dark periods, respectively. Samples were grown and incubated at high (HN, circles) and low nutrient (LN, triangles) conditions. Each symbol represents the mean of triplicate samples while the vertical lines indicate the standard deviation.

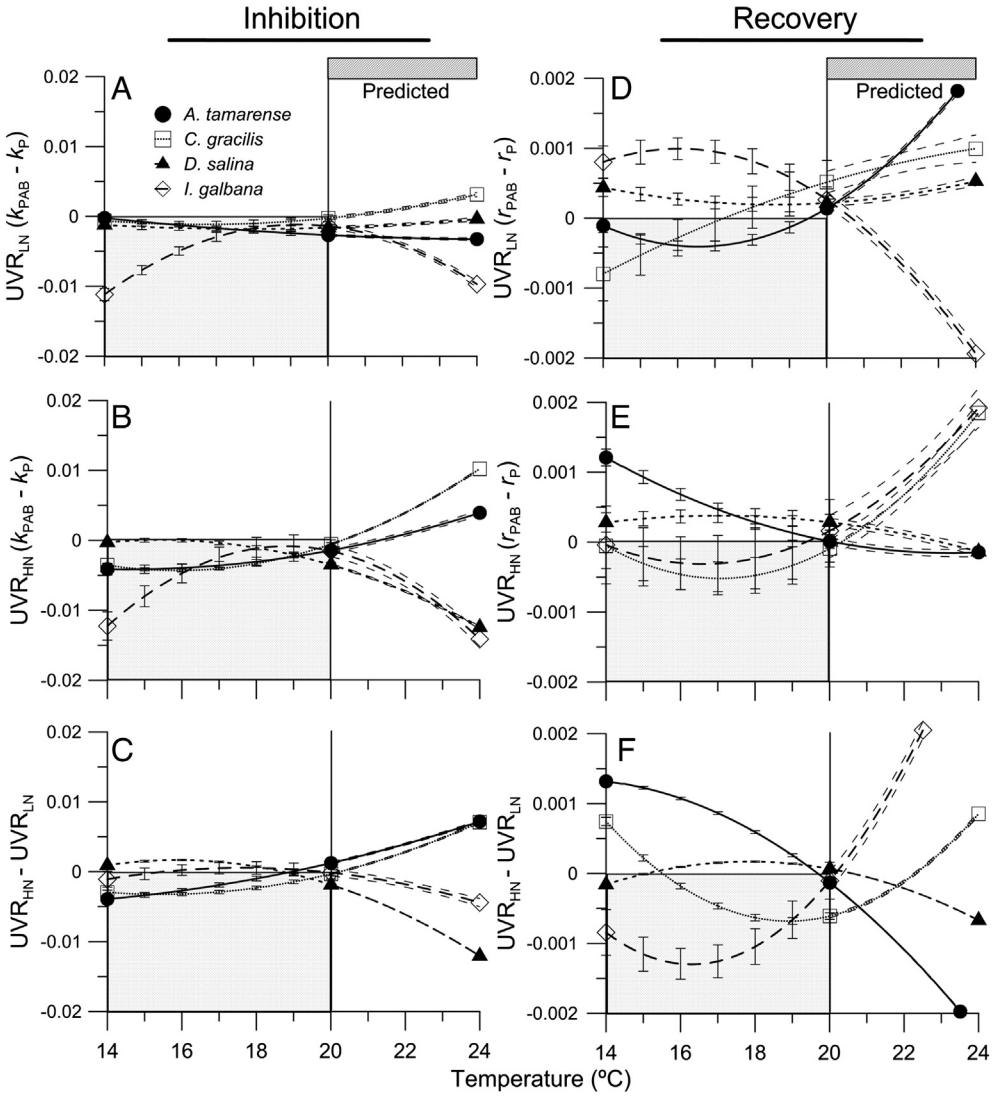

Fig. 7. UVR effect, evaluated as the difference between PAB and P treatments, on inhibition (A, B) (k) and recovery (D, E) (r) rates of *Alexandrium tamarense* (circles), *Chaetoceros gracilis* (squares), *Dunaliella salina* (triangles), and *Isochrysis galbana* (diamonds) within the experimental temperature interval (temperatures up to 20 °C) and within the increased temperature (i.e., predicted values, temperatures up to 24 °C). Samples were grown and incubated at high (HN) and low (LN) nutrient conditions, and three temperatures, 14, 17, and 20 °C. The net effect of high nutrients under UVR within the experimental (temperatures up to 20 °C) and increased temperature interval (i.e., predicted values, temperatures up to 24 °C) on inhibition (C) and recovery (F) is shown. The lines (solid and broken) represent the best fit using a polynomial function, while the vertical lines represent 95% confidence intervals, shown every 1 °C in the 14–20 °C interval, and continuously in the 20–24 °C interval.

samples under the P-treatment that had lower k values than when receiving UVR for both nutrient conditions in all species.

The net effect of UVR on k and r values as a function of temperature for the two nutrient conditions is shown in Fig. 7. As observed with photosynthesis, species-specific responses were found: UVR had a negative impact on PSII, increasing the inhibition rates in all species, regardless of the nutrient conditions, up to 20 °C (Fig. 7A, B, dotted area). At predicted increased temperatures it was found that: (i) Under LN conditions (Fig. 7A, striped bar), a synergistic effect of UVR and temperature was determined for *I. galbana* as with higher temperatures, inhibition rates increased. However, increasing temperatures had antagonistic effects with UVR counteracting its negative impact in *C. gracilis*. Increased temperature did not modify the UVR inhibitory effect in *A. tamarense* and *D. salina* (i.e., striped bar). (ii) Under HN conditions (Fig. 7B, striped bar), increased temperature enhanced the UVR inhibition (i.e., synergistic effect — dotted area) in *D. salina* and *I. galbana*, but it counteracted the negative UVR effects in *A. tamarense* and *C. gracilis*. Overall, a combination of increased temperature and nutrients will significantly counteract UVR inhibition in *A. tamarense* and *C. gracilis* but will enhance it in *I. galbana* and *D. salina* (Fig. 7C, striped bar).

In the case of r under LN conditions (Fig. 7D), increasing temperatures resulted in an increase in recovery for all species, with the exception of *I. galbana*, that presented an opposite effect. The addition of nutrients changed this pattern, with *C. gracilis* and *I. galbana* (Fig. 7E) benefiting from the increase in temperature and thus having higher recovery rates than under LN conditions. *A. tamarense* and *D. salina*, on the other hand, had in general a decrease of r as temperature increased. These patterns between LN and HN conditions resulted in an increased recovery capacity of *C. gracilis* and *I. galbana*, but not of *A. tamarense* and *D. salina*, under net increased nutrients and predicted temperature (Fig. 7F).

5. Discussion

The main goal of this study was to simultaneously evaluate the impact of multiple variables (i.e., UVR exposure, nutrient inputs and temperature) on photosynthetic responses and respiration of key

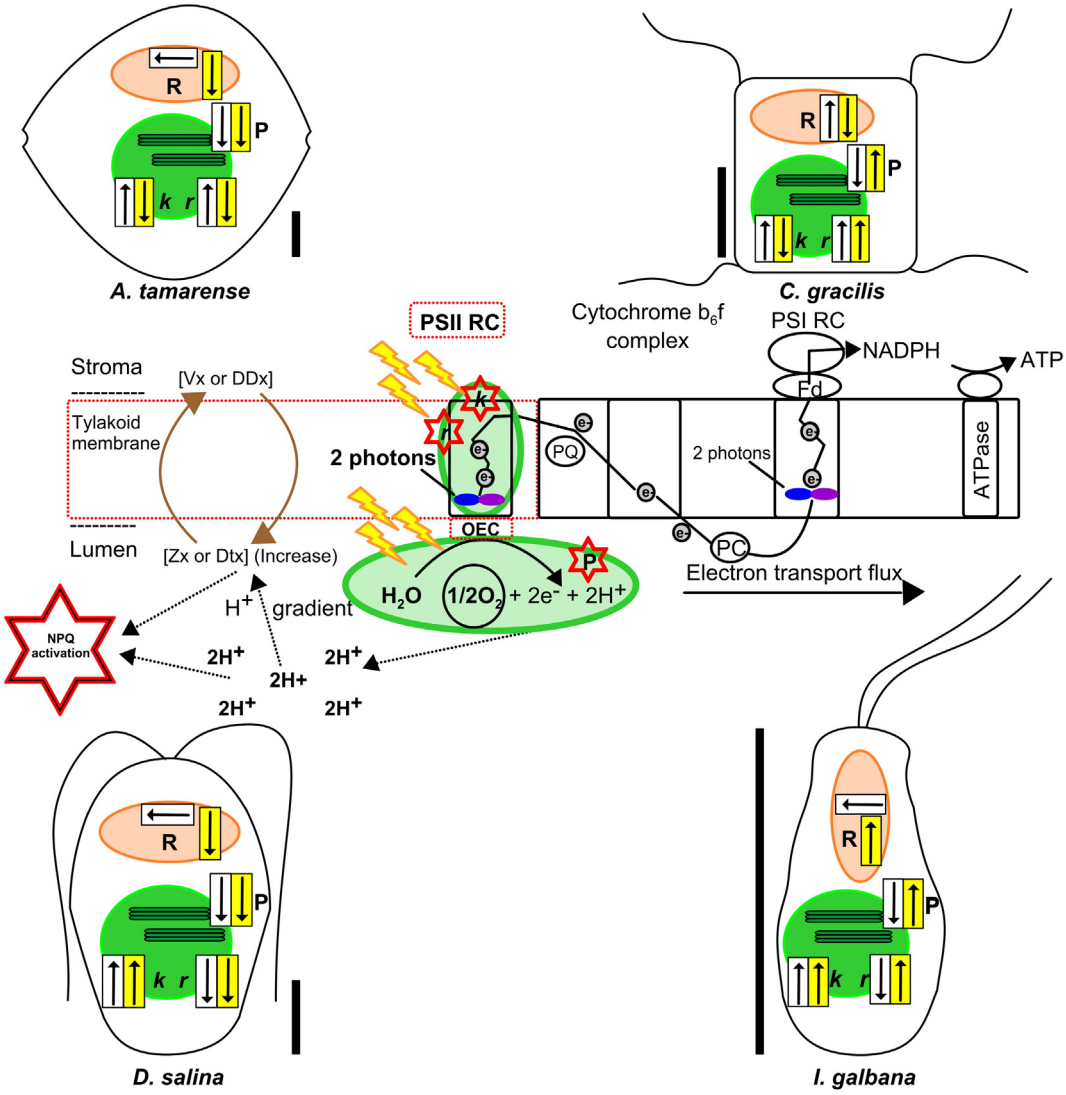

Fig. 8. Conceptual graphical model on the combined impact of UVR, nutrient inputs and increased temperature on photosynthetic and respiratory processes in *Alexandrium tamarense*, *Chaetoceros gracilis*, *Dunaliella salina* and *Isochrysis galbana*. Within each cell we represented a chloroplast (green), and a mitochondria (orange) and the processes evaluated in these organelles: photosynthesis (P), respiration (R), inhibition (*k*) and recovery (*r*) under current (white-rectangle with arrows) and predicted (yellow-rectangle with arrows) conditions of UVR, nutrients and temperature. The middle panel shows in detail the specific location and development of these processes, as well as the underlying-related mechanisms that are occurring in the photosystem II. The scale bar represents 5 μm.

phytoplankton species representative of four marine taxa found in estuarine and coastal waters. To the best of our knowledge, this is the first study that evaluated these responses considering both a current and a future environmental scenario in a context global change. Our study also highlights the importance of carrying out multifactorial experiments to better predict interactive effects among global change variables as well as their impact on aquatic organisms.

5.1. Current environmental scenario

Overall, our study shows a synergistic UVR-effect under current ambient conditions of relatively low nutrients and temperatures <20 °C (Fig. 8, white-rectangle arrows) as all species have a reduction in photosynthesis (Fig. 8, P). It has been reported that the oxygen evolving complex (OEC) seems to be UVR-sensitive, especially to UV-B (Kataria et al., 2014). Vass et al. (1996) measured the effects of UVR on different components of PSII, and found that OEC appeared to be the most sensitive, concluding that the primary damage by UVR occurs in this complex. In this sense, any damage in the OEC due to UVR would produce an alteration in the water-splitting reaction, triggering a decrease in photosynthesis (i.e., oxygen production) as shown in all of our species tested (Fig. 8, P; white-rectangle arrows). Besides, the decrease in photosynthesis was coupled with a strong inhibition in PSII (Fig. 8, *k*). Radiation damages the PSII, and the increase in PSII-photoinhibition could be due to: (i) a direct UVR-impact on PSII (i.e. increasing damage and decreasing repair rates) and (ii) an indirect consequence of an alteration in the OEC. Such alteration in the OEC could also produce a decrease in the proton gradient, which is involved in NPQ-activation (Lavaud et al., 2012), resulting in low NPQ values observed in all species under current conditions. This mechanism of dissipation of excess energy decreased in the four species tested, in almost all conditions as temperature increased. Similar results were obtained in other studies working with diatoms (Helbling et al., 2011; Li et al., 2012), and the decrease of NPQ with increasing temperature was related to increasing metabolic pathways (i.e., RUBISCO) resulting in a better utilization of radiation and thus reaching higher production (Helbling et al., 2011). The evaluation of the presence of UVACs (data not shown) revealed no significant amounts of these compounds in our experiments with the exception of a small peak in *A. tamarense*. These UVACs, which could help to mitigate the harmful effects produced by UVR, have been determined both

in isolated species (Hannach and Sigleo, 1998) as well as in phytoplankton communities (Oubelkheir et al., 2013) and have a well-known photoprotective role.

A slight synergistic effect of UVR on respiration (i.e., increase) was only observed in *C. gracilis* (Fig. 8, R) but not in the other three species. This lack of UVR effect on respiration rates was observed in other studies carried out with microalgae that suggested that respiration is not appreciably altered during short-term exposures to UVR (hours) due to a low damage or by relatively fast repair once the damage had occurred, therefore without a measurable signal (Heraud and Beardall, 2002; Larkum and Wood, 1993). However, the results obtained in our study partially agree (Fig. 8, R in *C. gracilis*) with those carried out by Beardall et al. (1994) who reported an enhancement in respiration rates after pre-exposure to high photon fluxes in two microalgae species.

5.2. Predicted global change scenario

Under predicted environmental conditions an antagonistic UVR-effect will be observed under increased concentrations of nutrients and higher temperatures (Fig. 8, yellow-rectangle arrows) as compared to current conditions. The changes included an increase in photosynthesis of *C. gracilis* and *I. galbana* (Fig. 8, P), whereas respiration will decrease in all species, except for *I. galbana*, probably due to an increase in metabolic oxygen demand with increasing temperature (Clarke, 2003) (Fig. 8, *r*). On the other hand, the combined effects of increasing nutrients and temperature would result in higher UVR inhibition of PSII in *D. salina* and *I. galbana* (Fig. 8, *k*), while recovery would diminish in *D. salina* and *A. tamarense* (Fig. 8, *r*).

Despite the variability in the responses among the studied species, our results suggest that under the expected global change scenario, diatoms (*C. gracilis*) and haptophytes (*I. galbana*) would be benefited as the combined impact of increasing Rad × Nut × Temp would improve both photosynthesis (i.e., increasing oxygen production) and photochemical performance (i.e., increasing repair rates). For dinoflagellates (*A. tamarense*), and while photosynthesis would decrease, the rate of photosynthetic inhibition would decrease as well, and this, in the short term, might be associated with the content of UVACs. In contrast, chlorophytes (*D. salina*) would be the most damaged group as predicted conditions would cause greater inhibition and an overall decrease in photosynthesis. This could be related to the fact that chlorophytes have a xanthophyll-cycle acquired through evolution based exclusively on Violaxanthin (Vx), whereas in the other groups it is based on Diadinoxanthin (Ddx) or even though they have low levels of the Vx cycle. The Vx-cycle comprises two de-epoxidations while the Ddx-cycle involves only one de-epoxidation (Goss and Jakob, 2010), and thus reduces the response time to cope with any damage. Besides, algae with Ddx-cycle can also synthesize the xantophylls of the Vx-cycle, but in both cases the pigments of the Vx-cycle can only be available when algae are illuminated for long-periods (Lohr and Wilhelm, 1999). This supports our view of their low acclimation capacity over short-term exposures under the expected environmental changes imposed in our experiments. In contrast, and as seen in Fig. 8, an increase in photosynthesis seems to be a consequence of a suitable functioning of OEC (e.g. by favoring the water-splitting), which could produce: (i) an increase in the proton gradient that will entail an activation of NPQ, dissipating the excess of energy received as heat and, (ii) an increase in electron gradient. Both gradients could indirectly explain the increase in photosynthesis observed and in the PSII-repair rates for *C. gracilis* and *I. galbana*.

The observed metabolic changes under UVR might also be a consequence of a faster response and higher tolerance of small species (*C. gracilis* and *I. galbana*) as compared to large cells, as observed when assessing the impact on photosynthesis (Helbling et al., 2001). Partially in agreement with our results, previous studies have found a beneficial temperature-effect in small-sized species (Daufresne et al., 2009; Halac et al., 2013), which also agrees with the temperature–size rule (Hessen et al., 2013). Besides, it cannot be discarded that part of the variability in the observed responses are also related to the nutrient conditions, as cell volume is also a major determinant of nutrient uptake (Tambi et al., 2009). Small cells have generally higher uptake affinities for nutrients as compared to large cells due to their higher surface area to volume quotient (Finkel et al., 2007).

In summary, it was found that an increase in nutrients and temperature will counteract the UVR-inhibition on photosynthesis and photochemical performance of two (i.e. diatoms and haptophytes) out of four groups of marine phytoplankton. Since the interaction between UVR, nutrients and temperature conditions has not been previously examined by experimental manipulation on different phytoplanktonic groups, it is clear that more research is necessary to fully understand the responses by primary producers in a scenario of global change. Modeling and experimental approaches such as these developed in this study would help to improve our understanding about the interactive effects of global change variables on key eco-physiological processes. Although the approach used in this study constitutes a simplification of the events occurring in nature, it could be considered a novel way to explore and evaluate the acclimation to the future global change in phytoplankton key groups. These changes would not only affect the photosynthesis and primary production in estuaries and coastal areas, but it might also influence trophic interactions since a future scenario under these conditions could favor differentially smaller size organism (diatoms and haptophytes) bloom-development in contrast to other larger size taxonomic groups.

Acknowledgments

We thank A. Banaszak (ICMyL, UNAM, Mexico) for her critical and helpful comments on this manuscript. We also thank Cooperativa Eléctrica y de Servicios de Rawson for providing building's infrastructure for the experiments, Campus de Excelencia Internacional del Mar (CeiMar) for financial support and V. Fiorda and I. Albarracín for their help with phytoplankton cultures. We thank the comments and suggestions of Dr. Shumway and of one anonymous reviewer that helped us to improve our manuscript. This work was supported by Agencia Nacional de Promoción Científica y Tecnológica — ANPCyT (PICT 2012-0271), Consejo Nacional de Investigaciones Científicas y Técnicas — CONICET (PIP No. 112-201001-00228), Ministerio de Ciencia e Innovación (CGL2011-23681) and the Spanish Goverment Fellowship "Formación de Profesorado Universitario", FPU12/01243 to MJC and Fundación Playa Unión. This work is in partial fulfillment of the Ph.D. thesis of MJC. This is Contribution No. 141 of Estación de Fotobiología Playa Unión. **[SS]**

References

Abo-Shady, A.M., El-Sheekh, M.M., El-Naggar, A.H., Abomohra, A.E.-F., 2008. Effect of UV-B radiation on growth, photosynthetic activity and metabolic activities of *Chlorococcum* sp. Ann. Microbiol. 58, 21–27.

Arts, M.T., Rai, H., 1997. Effects of enhanced ultraviolet-B radiation on the production of lipid, polysaccharide and protein in three freshwater algal species. Freshw. Biol. 38, 597–610.

Barbieri, E.S., Villafañe, V.E., Helbling, E.W., 2002. Experimental assessment of UV effects upon temperate marine phytoplankton when exposed to variable radiation regimes. Limnol. Oceanogr. 47, 1648–1655.

Beardall, J., Raven, J.A., 2004. The potential effects of global climate change on microalgal photosynthesis, growth and ecology. Phycologia 43, 26–40.

Beardall, J., Burger-Wiersma, T., Rijkeboer, M., Sukenik, A., Lemoalle, J., Dubinsky, Z., Fontvielle, D., 1994. Studies on enhanced post-illumination respiration in microalgae. J. Plankton Res. 16, 1401–1410.

Beardall, J., Berman, T., Markager, S., Martinez, R., Montecino, V., 1997. The effects of ultraviolet radiation on respiration and photosynthesis in two species of microalgae. Can. J. Fish. Aquat. Sci. 54, 687–696.

Bergmann, T., Richardson, T.L., Paerl, H.W., Pinckney, J.L., Schofield, O., 2002. Synergy of light and nutrients on the photosynthetic efficiency of phytoplankton populations from the Neuse River estuary, North Carolina. J. Plankton Res. 24, 923–933.

Buma, A.G.J., Boelen, P., Jeffrey, W.H., 2003. UVR-induced DNA damage in aquatic organisms. In: Helbling, E.W., Zagarese, H.E. (Eds.), UV Effects in Aquatic Organisms and Ecosystems. The Royal Society of Chemistry, Cambridge, pp. 291–327.
Carrillo, P., Delgado-Molina, J.A., Medina-Sánchez, J.M., Bullejos, F.J., Villar-Argaiz, M., 2008. Phosphorus inputs unmask negative effects of ultraviolet radiation on algae in a high mountain lake. Global Change Biol. 14, 423–439.
Clarke, A., 2003. Costs and consequences of evolutionary temperature adaptation. Trends Ecol. Evol. 18, 573–581.
Cloern, J.E., Foster, S.Q., Kleckner, A.E., 2014. Review: phytoplankton primary production in the world's estuarine–coastal ecosystems. Biogeosciences 11, 2477–2501.
Cruces, E., Huovinen, P., Gomez, I., 2013. Interactive effects of UV radiation and enhanced temperature on photosynthesis, phlorotannin induction and antioxidant activities of two sub-Antarctic brown algae. Mar. Biol. 160, 1–13.
Daufresne, M., Lengfellner, K., Sommer, U., 2009. Global warming benefits the small in aquatic ecosystems. Proc. Natl. Acad. Sci. U. S. A. 106, 12788–12793.
Dimier, C., Giovanni, S., Ferdinando, T., Brunet, C., 2009. Comparative ecophysiology of the xanthophyll cycle in six marine phytoplankton species. Protist 160, 397–411.
Field, C.B., Behrenfeld, M.J., Randerson, J.T., Falkowski, P.G., 1998. Primary production of the biosphere: integrating terrestrial and oceanic components. Science 281, 237–240.
Finkel, Z.V., Sebbo, J., Feist-Burkhardt, S., Irwin, A.J., Katz, M.E., Schofield, O.M.E., Young, J.R., Falkowski, P.G., 2007. A universal driver of macroevolutionary change in the size of marine phytoplankton over the Cenozoic. Proc. Natl. Acad. Sci. U. S. A. 104, 20416–20420.
Folt, C.L., Chen, C.Y., Moore, M.V., Burnaford, J.L., 1999. Synergism and antagonism among multiple stressors. Limnol. Oceanogr. 44, 864–877.
Genty, B.E., Briantais, J.M., Baker, N.R., 1989. The relationship between the quantum yield of photosynthetic electron transport and quenching of chlorophyll fluorescence. Biochim. Biophys. Acta 990, 87–92.
Goss, R., Jakob, T., 2010. Regulation and function of xantophyll cycle-dependent photoprotection in algae. Photosynth. Res. 106, 103–122.
Guihéneuf, F., Fouqueray, M., Mimouni, V., Ulmann, L., Jacquette, B., Tremblin, G., 2010. Effect of UV stress on the fatty acid and lipid class composition in two marine microalgae *Pavlova lutheri* (Pavlovophyceae) and *Odontella aurita* (Bacillariophyceae). J. Appl. Phycol. 22, 629–638.
Guillard, R.R.L., Ryther, J.H., 1962. Studies of marine planktonic diatoms. I. *Cyclotella nana* Husted, and *Detonula confervacea* (Cleve) Gran. Can. J. Microbiol. 8, 229–239.
Häder, D.-P., Helbling, E.W., Williamson, C.E., Worrest, R.C., 2011. Effects of UV radiation on aquatic ecosystems and interactions with climate change. Photochem. Photobiol. Sci. 10, 242–260.
Halac, S.R., Villafañe, V.E., Helbling, E.W., 2010. Temperature benefits the photosynthetic performance of the diatoms *Chaetoceros gracilis* and *Thalassiosira weissflogii* when exposed to UVR. J. Photochem. Photobiol. B Biol. 101, 196–205.
Halac, S.R., Guendulain-García, S.D., Villafañe, V.E., Helbling, E.W., Banaszak, A.T., 2013. Responses of tropical plankton communities from the Mexican Caribbean to solar ultraviolet radiation exposure and increased temperature. J. Exp. Mar. Biol. Ecol. 445, 99–107.
Hannach, G., Sigleo, A.C., 1998. Photoinduction of UV-absorbing compounds in six species of marine phytoplankton. Mar. Ecol. Prog. Ser. 174, 207–222.
Helbling, E.W., Zagarese, H.E., 2003. UV Effects in Aquatic Organisms and Ecosystems. The Royal Society of Chemistry, Cambridge (1–575 pp.).
Helbling, E.W., Santamarina, J.M., Villafañe, V.E., 1992. Chubut river estuary (Argentina): estuarine variability under different conditions of river discharge. Rev. Biol. Mar. 27, 73–90.
Helbling, E.W., Chalker, B.E., Dunlap, W.C., Holm-Hansen, O., Villafañe, V.E., 1996. Photoacclimation of antarctic marine diatoms to solar ultraviolet radiation. J. Exp. Mar. Biol. Ecol. 204, 85–101.
Helbling, E.W., Buma, A.G.J., de Boer, M.K., Villafañe, V.E., 2001. In situ impact of solar ultraviolet radiation on photosynthesis and DNA in temperate marine phytoplankton. Mar. Ecol. Prog. Ser. 211, 43–49.
Helbling, E.W., Gao, K., Gonçalves, R.J., Wu, H., Villafañe, V.E., 2003. Utilization of solar UV radiation by coastal phytoplankton assemblages off SE China when exposed to fast mixing. Mar. Ecol. Prog. Ser. 259, 59–66.
Helbling, E.W., Barbieri, E.S., Marcoval, M.A., Gonçalves, R.J., Villafañe, V.E., 2005. Impact of solar ultraviolet radiation on marine phytoplankton of Patagonia, Argentina. Photochem. Photobiol. 81, 807–818.
Helbling, E.W., Pérez, D.E., Medina, C.D., Lagunas, M.G., Villafañe, V.E., 2010. Phytoplankton distribution and photosynthesis dynamics in the Chubut River estuary (Patagonia, Argentina) throughout tidal cycles. Limnol. Oceanogr. 55, 55–65.
Helbling, E.W., Buma, A.G.J., Boelen, P., van der Strate, H.J., Fiorda Giordanino, M.V., Villafañe, V.E., 2011. Increase in Rubisco activity and gene expression due to elevated temperature partially counteracts ultraviolet radiation-induced photoinhibition in the marine diatom *Thalassiosira weissflogii*. Limnol. Oceanogr. 56, 1330–1342.
Heraud, P., Beardall, J., 2002. Ultraviolet radiation has no effect on respiratory oxygen consumption or enhanced post-illumination respiration in three species of microalgae. J. Photochem. Photobiol. B Biol. 68, 109–116.
Hessen, D.O., Daufresne, M., Leinaas, H.P., 2013. Temperature–size relations from the cellular-genomic perspective. Biol. Rev. 88, 476–489.
Holm-Hansen, O., Riemann, B., 1978. Chlorophyll a determination: improvements in methodology. Oikos 30, 438–447.
IPCC, 2013. Climate change 2013. The Physical Science Basis: Working Group I Contribution to the Fifth Assessment Report of the Intergovernmental Panel on Climate Change. Cambridge University Press, New York. USA (1552 pp.).
Kataria, S., Jajoo, A., Guruprasad, K.N., 2014. Impact of increasing ultraviolet-B (UV-B) radiation on photosynthetic processes. J. Photochem. Photobiol. B Biol. 137, 55–66.
Kennish, M.J., Brush, M.J., Moore, K.A., 2014. Drivers of change in shallow coastal photic systems: an introduction to a special issue. Estuar. Coasts 37, 3–19.
Korbee, N., Carrillo, P., Mata, M.T., Rosillo, S., Medina-Sánchez, J.M., Figueroa, F.L., 2012. Effects of ultraviolet radiation and nutrients on the structure–function of phytoplankton in a high mountain lake. Photochem. Photobiol. Sci. 11, 1087–1098.
Kulk, G., De Vries, P., Van de Poll, W., Ronald, J., Buma, A.G.J., 2013. Temperature-dependent photoregulation in oceanic picophytoplankton during excessive irradiance exposure. In: Dubinsky, Z. (Ed.), Photosynthesis. InTech, pp. 209–228 (http://www.intechopen.com/books/photosynthesis/temperature-dependent-photoregulation-in-oceanic-picophytoplankton-during-excessive-irradiance-expos).
Lagaria, A., Psarra, S., Lefèvre, D., Van Wanbeke, F., Courties, C., Pujo-Pay, M., Oriol, L., Tanaka, T.Y., Christaki, U., 2011. The effects of nutrient additions on particulate and dissolved primary production and metabolic state in surface waters of three Mediterranean eddies. Biogeosciences 8, 2595–2607.
Larkum, A.W.D., Wood, W.F., 1993. The effect of UV-B radiation on photosynthesis and respiration of phytoplankton, benthic macroalgae and seagrasses. Photosynth. Res. 36, 17–23.
Lavaud, J., Materna, A.C., Sturm, S., Vugrinec, S., Kroth, P.G., 2012. Silencing of the violaxanthin de-epoxidase gene in the diatom *Phaeodactylum tricornutum* reduces diatoxanthin synthesis and non-photochemical quenching. PLoS One 7, e36806.
Li, Y., Gao, K., Villafane, V.E., Helbling, E., 2012. Ocean acidification mediates photosynthetic response to UV radiation and temperature increase in the diatom *Phaeodactylum tricornutum*. Biogeosciences 9, 3931–3942.
Lohr, M., Wilhelm, C., 1999. Algae displaying the diadinoxanthin cycle also possess the violaxanthin cycle. Proc. Natl. Acad. Sci. U. S. A. 96, 8784–8789.
Luo, Y., Gerten, D., Le Maire, G., Parton, W.J., Weng, E., Zhou, X., Keough, C., Beier, C., Ciais, P., Cramer, W., Dukes, J.S., Emmett, B., Hanson, P.J., Knapp, A., Linder, S., Nepstad, D., Rustad, L., 2008. Modeled interactive effects of precipitation, temperature, and [CO_2] on ecosystem carbon and water dynamics in different climatic zones. Global Change Biol. 14, 1986–1999.
Maxwell, K., Johnson, G.N., 2000. Chlorophyll fluorescence — a practical guide. J. Exp. Bot. 51 (345), 659–668.
McKenzie, R., Aucamp, P.J., Bais, A., Björn, L.O., Ilyas, M., Madronich, S., 2011. Ozone depletion and climate change: impacts on UV radiation. Photochem. Photobiol. Sci. 10, 182–198.
Oubelkheir, K., Clementson, L., Moore, G.F., Tilstone, G.H., 2013. Production of mycosporine-like amino acids by phytoplankton under ultraviolet radiation exposure in the sub-Antarctic zone south of Tasmania. Mar. Ecol. Prog. Ser. 494, 41–63.
Porra, R.J., 2002. The chequered history of the development and use of simultaneous equations for the accurate determination of chlorophylls *a* and *b*. Photosynth. Res. 73, 149–156.
Skerratt, J.H., Davidson, A.D., Nichols, P.D., McMinn, T.A., 1998. Effect of UV-B on lipid content of three Antarctic marine phytoplankton. Phytochemistry 49, 999–1007.
Sobrino, C., Neale, P.J., 2007. Short-term and long-term effects of temperature on photosynthesis in the diatom *Thalassiosira pseudonana* under UVR exposures. J. Phycol. 43, 426–436.
Takahashi, S., Yoshioka-Nishimura, M., Nanba, D., Badger, M.R., 2013. Thermal acclimation of the symbiotic alga *Symbiodinium* spp. alleviates photobleaching under heat stress. Plant Physiol. 161, 477–485.
Tambi, H., Fonnes-Flaten, G.A., Egge, J.K., Bødtker, G., Jacobsen, A., Thingstad, T.F., 2009. Relationship between phosphate affinities and cell size and shape in various bacteria and phytoplankton. Aquat. Microb. Ecol. 57, 311–320.
Thomas, M.K., Kremer, C.T., Klausmeier, C.A., Litchman, E., 2012. A global pattern of thermal adaptation in marine phytoplankton. Science 338, 1085–1088.
Toseland, A., Daines, S.J., Clark, J.R., Kirkham, A., Strauss, J., Uhlig, C., Lenton, T.M., Valentin, K., Pearson, G.A., Moulton, V., Mock, T., 2013. The impact of temperature on marine phytoplankton resource allocation and metabolism. Nat. Clim. Chang. 3, 979–984.
Vass, I., László, S., Spetea, C., Bakou, A., Ghanotakis, D.F., Petrouleas, V., 1996. UV-B-induced inhibition of photosystem II electron transport studied by EPR and chlorophyll fluorescence. Impairment of donor and acceptor side components. Biochemistry 35, 8964–8973.
Winder, M., Sommer, U., 2012. Phytoplankton response to a changing climate. Hydrobiologia 698, 5–16.